Polarization effects in magnetic resonance: Application to a chainlike system

Etienne Bize, Sylvain Clément, and Jean-Pierre Renard
Institut d'Electronique Fondamentale, Bâtiment 220, Université Paris-Sud, 91405 Orsay, France
(Received 3 November 1987)

We present a theoretical and experimental study of "low-frequency" magnetic resonance. We show that the usual theory fails to correctly describe magnetic resonance, at frequencies of the order of the linewidth or smaller than the linewidth, in anisotropic systems. Bloch equations must be generalized in order to include two damping terms: one in the oscillating field polarization direction, and the other in the direction perpendicular both to the oscillating field and to the static field. These damping terms may be very different from each other. In particular, we focus on the case of a linear chain of spins with exchange and dipolar interactions, for which the damping is zero in the chain direction: Signal enhancement and line shift arise, especially when the oscillating field polarization axis is parallel to the chain axis, and such effects are strongly dependent to the polarization orientation. A microscopic theory based on the memory-function formalism which describes the polarization is fully given in this paper. It takes into account all nondiagonal terms of the frequency-dependent susceptibility tensor. For the linear chain it turns out that there is a perfect correspondence between phenomenologic theory and microscopic theory for two preferred orientations of the static field: parallel and perpendicular to the chain axis. This means that the relaxation of a total spin component can be considered as exponential for these orientations, with respective rates $1/T_{2c}=0$ and $1/T_{2t}$. We consider also the real case by taking into account phenomenologically interchain interactions ($1/T_{2c}\neq 0$). Experiments have been performed on the quasi-one-dimensional compound $(CH_3)_4NMnCl_3$ (TMMC), using a homemade spectrometer, at frequencies ranging between 25 and 225 MHz. All expected effects have been verified and we deduce the low-frequency–low-field damping $1/T_{2c}=5\times 10^8$ rad s^{-1} and $1/T_{2t}=10^{10}$ rad s^{-1}. For all field orientations, the line measurements are found in excellent agreement with the theory. Previous studies in TMMC are discussed in light of these results.

I. INTRODUCTION

It is well known that magnetic resonance phenomena result from the combined application to a paramagnetic sample of an oscillating magnetic field $\mathbf{B}_1$ and a static one $\mathbf{B}_0$. Usually the oscillating field is linearly polarized but one does not bother about the polarization direction, provided that the orthogonality condition be fulfilled ($\mathbf{B}_1\perp\mathbf{B}_0$). For the calculation of the resonance line it is convenient to split the oscillating field into two circularly polarized components and to neglect the effect of the "wrong" component that rotates reversely to the magnetic moments. This is, in fact, an approximation since the effect of a linearly polarized field cannot be, in general, reduced to the superposition of the effects produced by two rotating fields: an example is the multiquanta transitions occurrence when a strong $\mathbf{B}_1$ is applied. However, if we consider the linear response only, such phenomena do not appear. It can be shown, starting from Bloch equations, that the spectrum is then composed of a Lorentzian line centered at the Larmor frequency (ω_0) and another symmetrical one at $-\omega_0$, the "mirror" line, these lines being related to the above-mentioned circular components.

Thus it seems that a "superposition rule" holds for the linear response.[1] However, this result is only valid for an isotropic spin damping in the xy plane, perpendicular to the static field (supposed to be directed along $0z$); it is always assumed in the Bloch equations, i.e., same damping constant $1/T_2$ for the spin component along $0x$ and $0y$. This assumption does not hold for crystalline samples with anisotropic interactions. An example is given by a linear chain of spins. If the spins are coupled by isotropic Heisenberg exchange and anisotropic dipolar interactions, it turns out that the total spin component along the chain axis **c** is conserved: Indeed this component commutes with the secular part of the dipolar interaction, which means zero spin damping. Let us apply the oscillating field $\mathbf{B}_1$ in the chain direction; in the case of zero spin damping the absorption line profile is a δ function. In fact, one has also to apply a static field $\mathbf{B}_0$, perpendicular to $\mathbf{B}_1$, and thus to **c**: the spin component along **c** is no more a constant of motion since $\mathbf{B}_0$ induces a coupling between spin components via the Zeeman Hamiltonian. However, this spin damping decreases when B_0 is lowered so that the absorption line profile tends towards a δ function when $\omega\rightarrow 0$. The line is quite different for an oscillating field polarization perpendicular to the chain axis. A peculiar behavior is thus expected at low frequencies in such a system.

We have reported experimental evidence of this "polarization effect" in a previous paper.[2] We investigated the low-frequency electron spin-resonance spectrum in $(CH_3)_4NMnCl_3$ (TMMC) which is one of the most perfect one-dimensional magnetic compounds known to date. At high frequencies (X band) a small shift studied by Natsume *et al.*[3] is a remnant of the polarization effect.

It is the aim of the present paper to discuss in more de-

tail the polarization effect, theoretically and experimentally, showing that it dominates the magnetic resonance spectrum at "low" frequencies. By low frequencies we mean the frequencies of the order of (or smaller than) the spin damping terms in a sample.

Two theoretical approaches of these phenomena will be successively developed. In both cases we shall calculate the resonance line profile (linear response) of a system of coupled spins with magnetic moments $M_i = -\gamma\hbar\mathbf{S}_i$ (γ is the gyromagnetic ratio) for a given oscillating frequency ω, when the static field B_0 (conventionally directed along 0z) is varied. It is supposed here that all moments have the same gyromagnetic factor and though the calculation is implicitly made for electronic spins (in order to compare it with experiment), it is clear that it can be generalized to any kind of spin system. In this paper we consider the "high-temperature" case, i.e., $\hbar\omega \ll kT$ so that the line profile is directly related to the autocorrelation function[4] $G_\alpha(t)=\langle S_\alpha(t)S_\alpha(0)\rangle$, S_α being the projection of the total spin $\mathbf{S}$ onto the oscillating field $\mathbf{B}_1$; the angular brackets $\langle \cdots \rangle$ denote the statistical average. The absorption line is indeed proportional to the frequency Fourier transform of $G_\alpha(t)$.

Our first approach, which is described in Sec. II, is phenomenologic; the behavior of magnetic moments is described by means of macroscopic Bloch equations with different dampings acting upon spin components. By solving the system of Bloch equations, we obtain the line profile and the spin motion under the influence of fields.

A microscopic interpretation of the phenomena is given in Sec. III. The starting equation is the equation of motion of spin operators, involving the Hamiltonian of the system. The resonance line profile is rigorously obtained by taking into account all cross-correlation terms which are usually neglected.[5] The polarization effects described above arise in fact from some of these terms.

In Sec. IV these results are applied to a linear chain of spins since considerable effects are expected for such a system. Interchain interactions which remove the divergence of the line at low frequencies are considered. We also studied the longitudinal relaxation, the oscillating field now being parallel to the static field. This is not, of course, a polarization effect but anisotropic damping is also shown with this configuration.

Section V is devoted to the experimental setup, especially to a detailed description of the sensitive magnetic resonance spectrometer which was used for the low-frequency experiments. In Sec. VI we present experimental data obtained at room temperature in TMMC, giving evidence of the effects discussed previously. Finally, Sec. VII contains the summary and conclusions of the work.

II. PHENOMENOLOGICAL INTERPRETATION

A. The line profile

We want to find the resonance line profile within the linear-response approximation. In this case it does not depend on the spin-lattice relaxation time, nor on the oscillating field amplitude B_1. However, it may be a function of the field polarization. We thus write the following set of generalized Bloch equations, with different spin-damping parameters:

$$\frac{dS_x}{dt} = -\omega_z S_y(t) - \frac{S_x(t)}{T_{2x}} ,$$
$$\frac{dS_y}{dt} = -\omega_z S_x(t) - \frac{S_y(t)}{T_{2y}} . \tag{1}$$

For convenience the static field is expressed into the angular frequency unit $\omega_z = \gamma B_0$.

Let us take the oscillating field polarization along the x direction. We know that the time-averaged power at (angular) frequency is, for high temperatures $\hbar\omega \ll kT$, proportional to the Fourier transform of the correlation function $G_x = \langle S_x(t)S_x(0)\rangle$. However it is more convenient to consider the Laplace transform (with $p = i\omega$) of $G_x(t)$, $\Gamma_x(\omega)$. The real part of this function, $\Gamma'_x(\omega)$, is the physical quantity directly related to the absorption line.

In the isotropic case ($T_{2x} = T_{2y} = T_2$), it is known that the spectrum is composed to two Lorentzian lines, such that

$$\Gamma'_x(\omega) = \langle S_x^2\rangle \frac{1}{2T_2}\left[\frac{1}{(\omega-\omega_z)^2+\frac{1}{T_2^2}} + \frac{1}{(\omega+\omega_z)^2+\frac{1}{T_2^2}}\right] , \tag{2}$$

with $\langle S_x^2\rangle = NS(S+1)/3$, N being the number of ions with spin S.

In this section, for the sake of clarity, the damping is supposed to be field independent. In fact, it can be a complex function of the static field, giving rise to a non-Lorentzian line and to a "dynamic shift."

Indeed the mirror line resonating at $\omega_z = -\omega$ can be neglected for $\omega \gg 1/T_2$. One observed the usual resonance line at a field $\omega_z \simeq \omega$, its "width"—defined as the half-linewidth at half-amplitude—being $\Delta\omega = 1/T_2$. The same result is obtained for any oscillating field polarization in the $x0y$ plane.

Now let us consider the $1/T_{2x} = 0$ case. Our problem is more easily solved by multiplying Eqs. (1) by $S_x(0)$, performing the statistical average in order to get the wanted correlation function and then taking the Laplace transform. We obtain

$$\Gamma'_x(\omega) = \langle S_x^2\rangle \frac{1}{T_{2y}} \frac{\omega_z^2}{(\omega_z^2-\omega^2)^2+(\omega^2/T_{2y}^2)} . \tag{3}$$

The spectrum for the "perpendicular configuration," i.e., B_1 being directed along $0y$, is obtained following the same method,

$$\Gamma'_y(\omega) = \Gamma'_x(\omega)\frac{\omega^2}{\omega_z^2} . \tag{4}$$

The two configurations give similar results only in the high-frequency range ($\omega T_{2y} \gg 1$) since $\omega \simeq \omega_z$, the spin

components being strongly coupled by the high fields near resonance. As a consequence, the lines are Lorentzian (except far away in the wings), but with a linewidth of $1/2T_{2y}$. One can say that the rotation is so fast that the spins experience an isotropic damping which is the mean value of the real damping in the x and y directions.

As the frequency is lowered, several effects occur in relation to the value of the parameter $\delta=(\omega T_{2y})^{-1}$. A completely different behavior will be observed, as we are considering the "parallel line" $\Gamma'_x(\omega,\omega_z)$ or the "perpendicular line" $\Gamma'_y(\omega,\omega_z)$.

The first effect to be observed (even for low values of δ) is an asymmetry of the line: in the parallel configuration the low-field peak of the line derivation is larger than the high-field peak. This is because the absorption is zero at zero field. The opposite deformation is found for the perpendicular configuration.

A second-order effect is a line shift which occurs only for Γ'_x, the corresponding line taking its maximum at a field such that

$$\omega_z^4=\omega^4+\frac{\omega^2}{T_{2y}^2} . \tag{5}$$

It should also be noted that, in the isotropic case [Eq. (2)], there is a shift resulting from the superposition of the main line and the mirror line: the maximum is thus shifted towards low fields, according to the relation $\omega_z^2=\omega^2-(1/T_2^2)$.

In the low-frequency case ($\omega T_{2y}\ll 1$), the most remarkable feature is the large enhancement of Γ'_x, in connection with a narrowing of the line. At resonance, Γ'_x has a value which is nearly independent of the damping term

$$\Gamma'_x=\frac{\langle S_x^2\rangle}{2\omega} \tag{6}$$

and the line would tend towards a δ function as $\omega\to 0$. We can approximate this behavior since at zero field S_x is a constant of motion and Γ'_x becomes then singular. Of course there is no divergence of the rf absorbed power since this last quantity is, in fact, proportional to $\omega^2\Gamma'_x(\omega)$, one ω term coming from the induction law and the other one from the Boltzmann factor.

The perpendicular line suffers no such variations, being always maximum at the Larmor value $\omega_z=\omega$, with the value $\Gamma'_y=\langle S_x^2\rangle T_{2y}$. However, its width becomes comparable to the parallel line value $\Delta\omega\sim(\omega/T_{2y})^{1/2}$. The Larmor value is indeed remarkable since the absorption is then isotropic,

$$\Gamma'_x(\omega_z=\omega)=\Gamma'_y(\omega_z=\omega) .$$

A graphic illustration of these effects is given in Fig. 1.

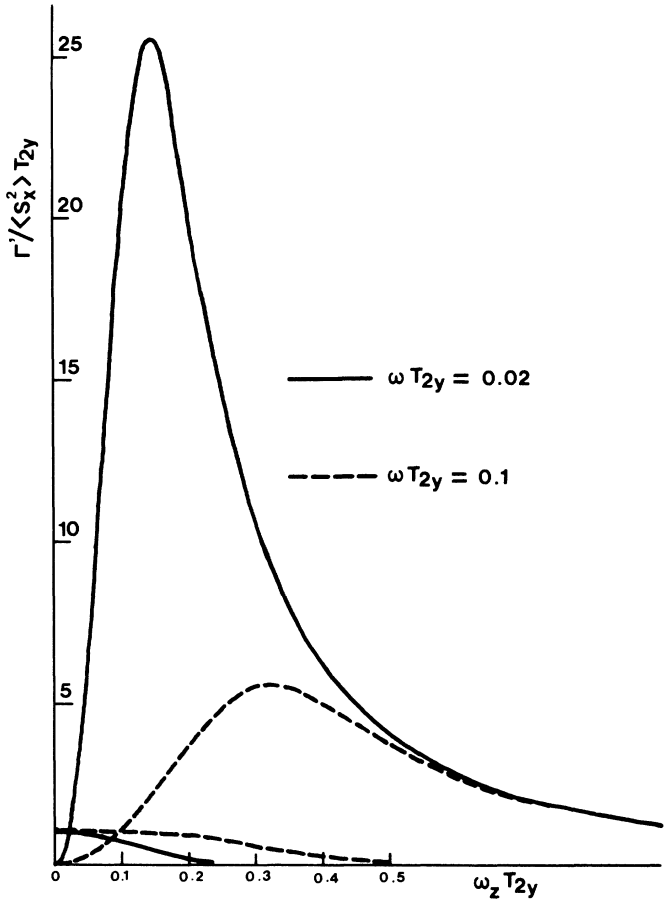

FIG. 1. Magnetic resonance lines for two oscillating field orientations. The static field is applied in the z direction. The damping along $0x$ is $1/T_{2x}=0$ and the damping along $0y$ is $1/T_{2y}$. Upper lines: The oscillating field $\mathbf{B}_1$ is applied along $0x$. Lower lines: $\mathbf{B}_1$ is applied along $0y$. The lines are calculated in reduced units from Eqs. (3) and (4).

If we now solve the general case ($1/T_{2x}\neq 0$) with the same method, we obtain

$$\Gamma'_x=\langle Sx^2\rangle\frac{\frac{1}{T_{2y}}[\omega_z^2+(1/T_{2x}T_{2y})]+\frac{\omega^2}{T_{2x}}}{[\omega_z^2-\omega^2+(1/T_{2x}T_{2y})]^2+\omega^2[(1/T_{2x})+(1/T_{2y})]^2} , \tag{7}$$

and a similar result for Γ'_y with the parameters T_{2x} and T_{2y} being interchanged. It is interesting to examine the influence of a small $1/T_{2x}$ on the polarization effect described above. We can see from (7) that at low frequencies, the line spectrum is again described by (3) but with the field ω_z being replaced by an "effective field"

$$\omega'_z=\left[\omega_z^2+\frac{1}{T_{2x}T_{2y}}\right]^{1/2} .$$

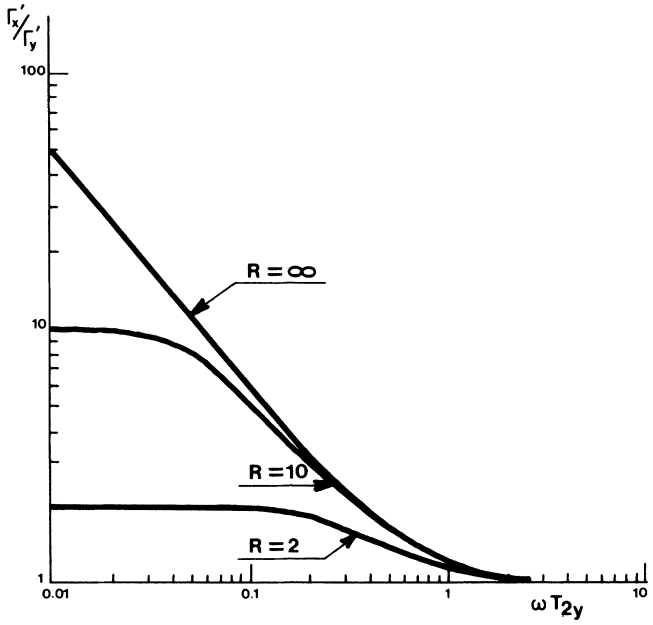

FIG. 2. Ratio of the resonance signals in the parallel ($\mathbf{B}_1 \| 0x$) and in the perpendicular ($\mathbf{B}_1 \| 0y$) configuration, plotted vs the frequency in reduced units.

If $\omega \leq 1/T_{2x}$ the line amplitude is reduced and is maximum at zero field. At higher frequencies the resonance field now corresponds to

$$\omega_z^2 \simeq \frac{1}{T_{2y}} \left[\omega - \frac{1}{T_{2x}} \right] , \tag{8}$$

but a remarkable feature is that the line maximum is again approximately given by Eq. (6). In any case the polarization effect may be observed but the line enhancement is limited to a value (T_{2x}/T_{2y}) (see Fig. 2).

B. The spin motion

We consider now the time resolution of the Bloch equations, the oscillating field and the longitudinal relaxation being included. These equations are

$$\frac{dS_x}{dt} = -\omega_z S_y - S_x/T_{2x} ,$$

$$\frac{dS_y}{dt} = \omega_z S_x - (S_y/T_{2y}) - \omega_1 S_z \cos(\omega t) ,$$

$$\frac{dS_z}{dt} = \omega_1 S_y \cos(\omega t) + (\langle S_z \rangle - S_z)/T_1 ,$$

with $\omega_1 = \gamma B_1$, the field $B_1 \cos(\omega t)$ being directed along the x direction.

The usual way of resolution[6] consists of expanding a component S_α as in the following:

$$S_\alpha(t) = {}^{(0)}S_\alpha + \omega_1 {}^{(1)}S_\alpha + \omega_1^2 {}^{(2)}S_\alpha + \ldots$$

so that new differential equations involving ${}^{(n)}S_\alpha$ are obtained. Then the ${}^{(n)}S_\alpha$ are obtained as a series of Fourier components

$${}^{(n)}S_\alpha = \sum_{m=-\infty}^{+\infty} {}^{(n)}_{m}S_\alpha e^{im\omega t} .$$

The coefficients of the development ${}^{(n)}_{m}S_\alpha$ are obtained by identification of ω_1^n and $e^{im\omega t}$ terms; since S_α is real one has ${}^{(n)}_{-m}S_\alpha = ({}^{(n)}_{m}S_\alpha)^*$. In the steady state ($n=0$) the spin components are zero except ${}^{(0)}_{0}S_z = \langle S_z \rangle = S_0$, i.e., the spin polarization along the static field. If we consider then the linear response ($n=1$) we have

$${}^{(1)}_{1}S_z = 0 ,$$

$${}^{(1)}_{1}S_y = \frac{S_0}{2} \frac{[i\omega + (1/T_{2x})]}{[i\omega + (1/T_{2y})][i\omega + (1/T_{2x})] + \omega_z^2} ,$$

$${}^{(1)}_{1}S_x = {}^{(1)}_{1}S_y \frac{\omega_z}{[i\omega + 1/T_{2x}]} .$$

$S_x(t)$ and $S_y(t)$ can be written as ($a\cos\omega t + b\sin\omega t$), the parameters a and b depending on the field and the damping terms. So, in general, the resulting motion of the spin projection in the xy plane is elliptic. However the motion becomes approximately circular at resonance, when $\omega \gg 1/T_2$, for the isotropic case

$$S_y(t) \simeq \tfrac{1}{2}\omega_1 S_0 T_2 \cos(\omega t) ,$$

$$S_x(t) \simeq \tfrac{1}{2}\omega_1 S_0 T_2 \sin(\omega t) .$$

Now, if we again consider the case $1/T_{2x} = 0$, we obtain

$$S_x(t) = \omega_1 S_0 \frac{\omega_z}{(\omega_z^2 - \omega^2)^2 + (\omega^2/T_{2y}^2)} \times \left[(\omega_z^2 - \omega^2)\cos(\omega t) + \frac{\omega}{T_{2y}} \sin(\omega t) \right] ,$$

$$S_y(t) = \omega_1 S_0 \frac{\omega}{(\omega_z^2 - \omega^2)^2 + (\omega^2/T_{2y}^2)} \times \left[\frac{\omega}{T_{2y}} \cos(\omega t) - (\omega_z^2 - \omega^2)\sin(\omega t) \right] .$$

The motion is also circular at Larmor frequency ($\omega_z = \omega$). A quite different motion occurs at resonance ($\omega_z^2 \simeq \omega/T_{2y}$) in the low-frequency case, as is shown in Fig. 3. It corresponds to

$$S_x(t) = \tfrac{1}{2}\omega_1 S_0 (T_{2y}/\omega)^{1/2} [\cos(\omega t) + \sin(\omega t)] ,$$

$$S_y(t) = \tfrac{1}{2}\omega_1 S_0 T_{2y} [\cos(\omega t) - \sin(\omega t)] .$$

The extremity of the vector $\mathbf{S}$ describes an ellipse with ellipticity $(\omega T_{2y})^{1/2}$. It is seen here that the spin polarization in the xy plane is mostly near the x direction.

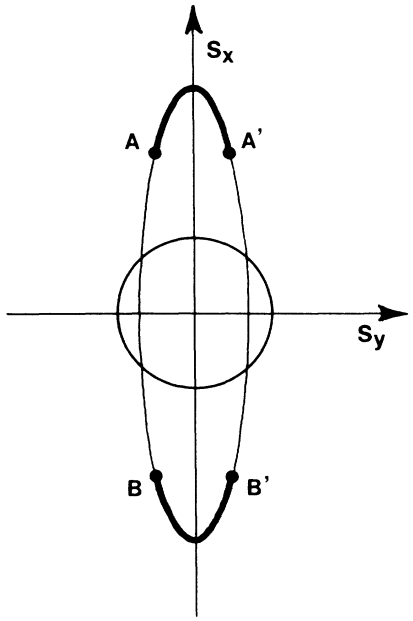

FIG. 3. Spin motion projected onto the $x0y$ plane, in the case $\omega T_{2y}=0.05$. The static field is directed along 0z and the oscillating field is directed along 0x. The circle represents the motion at the Larmor frequency; the ellipse represents the motion at resonance. The spin spends half the time between *A-A'* and *B-B'* (heavy lines).

III. MICROSCOPIC INTERPRETATION

Electron spin-resonance spectra are usually described by means of the Kubo-Tomita theory. However this theory breaks down in some cases. A first example concerns systems for which time-dependent spin correlation functions decrease very slowly, such as in low-dimensional systems where spin dynamics are characterized by diffusion.[7] A description within the "memory function" formalism (or Mori formalism) becomes necessary.[8] Another limit of the validity of the Kubo-Tomita theory is reached when the oscillating frequency has a value comparable to the linewidth. The reason is that the theory does not take into account nondiagonal components of the susceptibility tensor. This fact was clearly recognized by Kubo and Tomita themselves[4] and more recently by Lagendijk.[9] However, the correction terms were not considered until recently since they are negligible in almost all cases while the calculations are complicated. The question was raised by Natsume *et al.*[3] who observed at the *X* band in quasi-one-dimensional TMMC an anomalous shift depending on the azimuthal angle φ (the angle between the oscillating field and the plane defined by the static field and the chain axis).

In this section we want to obtain a rigorous expression of the magnetic resonance spectrum (linear response) of a spin system with Hamiltonian H. For convenience, in the following, the static field ($\omega_z=\gamma B_0$) the Hamiltonian, and other terms of interest (linewidth, line shift) will often be expressed in angular frequency units. The system is first supposed to be submitted to an oscillating field $\mathbf{B}_1(t)=\mathbf{B}_1\cos(\omega t)$ directed along the x direction, the static field being, as usual, parallel to the z axis.

The general theory of Kubo-Tomita[4] shows that the mean power absorbed by the sample is, in the limit of high temperatures ($\hbar\omega \ll kT$, k being the Boltzmann constant), proportional to the real part Γ'_x of the Laplace transform of the autocorrelation function of the total spin component S_x,

$$\Gamma_x(\omega)=\int_0^\infty \langle S_x(0)S_x(t)\rangle e^{-i\omega t}dt \ . \tag{9}$$

It is convenient to introduce the ladder operators $S_\pm=S_x\pm iS_y$.

If we put down $G_{\alpha\beta}(t)=\langle S_\alpha(0)S_\beta(t)\rangle$ and its Laplace transform $\Gamma_{\alpha\beta}(\omega)$ ($\alpha,\beta=z,+,-$) we get

$$\Gamma_x(\omega)=\tfrac{1}{4}[\Gamma_{+-}(\omega)+\Gamma_{--}(\omega)+\Gamma_{-+}(\omega)+\Gamma_{++}(\omega)] \ . \tag{10}$$

In the usual theory it is of common practice to neglect correlations terms which are zero at zero time (G_{--} and G_{++}). Actually, a derivation taking into account all these terms can be performed. Details of the calculation are given in the Appendix. The absorption profile is a function of nine complex terms labeled a_i, b_j, c_k ($i,j,k=1,2,3$). Among these, only three terms, a_1, a_2, a_3, are considered by usual theory. One obtains

$$\Gamma_x=\frac{\langle S_x^2\rangle}{2}\frac{n}{d} \tag{11}$$

with

$$n=a_3(a_1+a_2+b_1+c_2)+(b_2-c_1)(b_3-c_3) \ . \tag{12}$$

d can be written as a determinant

$$d=\begin{vmatrix} a_1 & c_2 & b_3 \\ b_1 & a_2 & -c_3 \\ c_1 & -b_2 & a_3 \end{vmatrix} \ . \tag{13}$$

Another field configuration is interesting, the so-called "relaxation configuration," corresponding to an oscillating field applied along the z axis, i.e., parallel to the static field. For such a case Eqs. (9) and (10) are valid with the proviso that S_x is replaced by S_z. We get

$$\Gamma_z(\omega)=\langle S_z^2\rangle\frac{n'}{d} \tag{14}$$

with

$$n'=a_1a_2-b_1c_2 \ . \tag{15}$$

We have obtained compact expressions for the magnetic resonance absorption, which are exact in the limit of linear response and for high-temperature conditions. It should be added that extension to low temperatures is possible through the use of Kubo transforms[10] instead of correlation functions.

The a,b,c terms are expressed as functions of memory functions $K_{\alpha\beta}(\omega,\omega_z)$ and of characteristic frequencies

$\omega_{\alpha\beta}$, given in the Appendix. In fact, at high temperatures, static shifts resulting from anisotropic spin-spin interactions may be ignored so that all terms $\omega_{\alpha\beta}$ are negligible except $\omega_{+-}=-\omega_z$ and $\omega_{-+}=\omega_z$.

The terms $K_{\alpha\beta}$ are at most of the order of the linewidth, so that the terms a_1, a_2, and a_3 are predominant. Taking $\omega_z>0$ we thus have

$$\Gamma_x(\omega,\omega_z)\simeq\Gamma_{-+}\simeq\frac{\langle S_x^2\rangle}{2}\frac{1}{i(\omega-\omega_z)+K_{-+}(\omega,\omega_z)} \quad (16)$$

which is the relation used for the description of the high-frequency spectrum of TMMC. It corresponds to the case $\omega T_2\gg 1$ defined in Sec. II. In the same way the high-frequency relaxation profile is given by

$$\Gamma_z(\omega,\omega_z)\simeq\frac{\langle S_z^2\rangle}{a_3}=\frac{\langle S_z^2\rangle}{i\omega+K_{zz}(\omega,\omega_z)} . \quad (17)$$

The relaxation of S_z towards its equilibrium value is usually nearly exponential with a time constant T_1,

$$\langle S_z(0)S_z(t)\rangle=\langle S_z^2\rangle e^{-t/T_1} ,$$

with

$$T_1(\omega_z)=K_{zz}(\omega=0,\omega_z) . \quad (18)$$

One can also consider the case of a spin Hamiltonian of axial symmetry, so that the S_z component is conserved. This situation occurs for a linear chain of spins when the static field is parallel to the chain axis. Symmetry considerations show that

$$\Gamma_x=\frac{\langle S_x^2\rangle}{2}\left[\frac{1}{a_1}+\frac{1}{a_2}\right] \quad (19)$$

for all frequencies. Of course there are no polarization effects in this case.

IV. APPLICATION TO A LINEAR CHAIN OF SPINS

A. General formulation of the spectrum

In this section we shall consider the case of a linear chain of spins corresponding to the experimental case of tetramethylammonium manganese chloride (TMMC). At this stage, interchain interactions and spin-lattice relaxation are ignored. The spin Hamiltonian is the sum of three terms: the Heisenberg exchange term $H_{ex}=-2J\sum_i \mathbf{S}_i\cdot\mathbf{S}_{i+1}$, the Zeeman term $H_Z=\omega_z S_z$, and the dipolar term H_D which can be split[4] according to the value of the total magnetic number M ($M=0,\pm1,\pm2$) as in the following:

$$H_D=\sum_M D_M=\sum_M\sum_{ij}F_{ij}^M A_{ij}^M \quad (i\neq j) .$$

Accordingly, the Liouville operator can be written as

$$L=L_{ex}+L_Z+L_D .$$

The memory function $k_{\alpha\beta}(t)$ is given by Eq. (A5) in the Appendix:

$$k_{\alpha\beta}(t)=\langle[H_D,S_\alpha]e^{i(1-P)Lt}[S_\beta,H_D]\rangle/\langle S_\beta S_\beta\rangle .$$

We then have correlation functions of the form

$$\varphi_{MM'}(t)=\langle A_{ij}^M e^{i(1-P)Lt}A_{kl}^{M'}\rangle .$$

The main difficulty is in the calculation of these functions, which is complicated by the presence of the projector in the propagator. In fact, here, the exchange term is usually strongly prevailing so that approximations can be made. Symmetry properties of H_{ex} also allow simplifications. All correlation functions are disregarded if $M+M'=0$. The effects of operators P and H_D are noticeable essentially at long times, when the diffusive process resulting from the conservation of total spin by H_{ex} is damped by dipolar interactions. The simplest approximation consists in representing phenomenologically this mechanism by an exponential damping term[11,12] (but other functional forms may be chosen):

$$e^{i(1-P)Lt}\approx e^{i(L_{ex}+L_z)t}e^{-\omega_c t} . \quad (20)$$

The cutoff frequency ω_c is then evaluated when possible. In quasiperfect one-dimensional (1D) systems such as TMMC, the same (dipolar) interactions are responsible for both the line broadening and cutoff mechanism, so that the linewidth and cutoff frequency are closely related: $\omega_c\sim\Delta\omega$; ω_c is generally dependent on the orientation and magnitude of the static field. The effect of the Zeeman operator can be factorized as

$$\langle A_{ij}^M e^{i(L_{ex}+L_z)t}A_{kl}^{-M}\rangle=\langle A_{ij}^M e^{iLext}A_{kl}^{-M}\rangle e^{-iM\omega_z t}$$
$$\equiv\langle A_{ij}^M A_{kl}^{-M}(t)\rangle e^{-iM\omega_z t} , \quad (21)$$

the time dependence of A_{kl}^{-M} now being governed solely by H_{ex}. From rotational symmetry it has been shown[11] that this time dependence is the same for all M values. For the cutoff zone, this point will be cleared up later. For the moment we cautiously define a particular ω_c^M for every type of function.

The memory functions [which are such that $k_{\alpha\beta}^*(t)=k_{\alpha^*\beta^*}(t)$] are given in terms of correlation functions

$$\varphi_M(t)=\varphi_{KT}(t)e^{-i\omega_c^M t} , \quad (22)$$

$$\varphi_{KT}(t)=\sum_{\substack{i,j,k,l\\ i\neq j\\ k\neq l}}|i-j|^{-3}|k-1|^{-3}\times\frac{\langle S_i^+S_j^+S_k^-(t)S_l^-(t)\rangle}{\langle S_+S_-\rangle} , \quad (23)$$

being the bulk function occurring within the Kubo-Tomita theory[12] ($\mathbf{S}_i$ is the spin at site i and $S_i^\pm$ has its usual significance).

Resultant expressions for the a,b,c terms can be obtained from the Laplace transform of $\varphi_M(t)$, $\phi_M(\omega)$ and the known dipolar coefficients. They are listed in Table I. The dipolar frequency corresponds to $\hbar\gamma^2/c^3$ where c is the smallest separation between two ions in the chain. The chain axis $\mathbf{c}$ is defined by spherical coordinates

TABLE I. Theoretical expressions of the line-shape parameters for the linear chain case.

$$a_1 = i(\omega+\omega_z)+(\tfrac{9}{16})\omega_D^2\{(1-3\cos^2\theta)^2\phi_1(\omega+\omega_z) + (\sin^2\theta\cos^2\theta)[6\phi_0(\omega)+4\phi_2(\omega+2\omega_z)]+(\sin^4\theta)\phi_1(\omega-\omega_z)\}$$

$$a_2 = i(\omega-\omega_z)+(\tfrac{9}{16})\omega_D^2\{(1-3\cos^2\theta)^2\phi_1(\omega-\omega_z) + (\sin^2\theta\cos^2\theta)[6\phi_0(\omega)+4\phi_2(\omega-2\omega_z)]+(\sin^4\theta)\phi_1(\omega+\omega_z)\}$$

$$a_3 = i\omega+(\tfrac{9}{16})\omega_D^2\{(2\sin^2\theta\cos^2\theta)[\phi_1(\omega+\omega_z)+\phi_1(\omega-\omega_z)] + (2\sin^4\theta)[\phi_2(\omega+2\omega_z)+\phi(\omega-2\omega_z)]\}$$

$$b_1 = (\tfrac{9}{16})\omega_D^2 e^{2i\varphi}[(1-3\cos^2\theta)(\sin^2\theta)[\phi_1(\omega+\omega_z)+\phi_1(\omega-\omega_z)] + (6\sin^2\theta\cos^2\theta)\phi_0(\omega)]$$

$$b_2 = (\tfrac{9}{16})\omega_D^2 e^{-i\varphi}[2(1-3\cos^2\theta)(\sin\theta\cos\theta)\phi_1(\omega-\omega_z) - (4\sin^3\theta\cos\theta)\phi_2(\omega-2\omega_z)-(2\sin^3\theta\cos\theta)\phi_1(\omega+\omega_z)]$$

$$b_3 = (\tfrac{9}{16})\omega_D^2 e^{-i\varphi}[(1-3\cos^2\theta)(\sin\theta\cos\theta)\phi_1(\omega+\omega_z) - (2\sin^3\theta\cos\theta)\phi_2(\omega+2\omega_z)-(\sin^3\theta\cos\theta)\phi_1(\omega-\omega_z)]$$

$$c_1 = (\tfrac{9}{16})\omega_D^2 e^{i\varphi}[2(1-3\cos^2\theta)(\sin\theta\cos\theta)\phi_1(\omega+\omega_z) - (4\sin^3\theta\cos\theta)\phi_2(\omega+2\omega_z)-(2\sin^3\theta\cos\theta)\phi_1(\omega-\omega_z)]$$

$$c_2 = (\tfrac{9}{16})\omega_D^2 e^{-2i\varphi}\{(1-3\cos^2\theta)(\sin^2\theta)[\phi_1(\omega+\omega_z)+\phi_1(\omega-\omega_z)] + (6\sin^2\theta\cos^2\theta)\phi_0(\omega)\}$$

$$c_3 = (\tfrac{9}{16})\omega_D^2 e^{i\varphi}[(1-3\cos^2\theta)(\sin\theta\cos\theta)\phi_1(\omega-\omega_z) - (2\sin^3\theta\cos\theta)\phi_2(\omega-2\omega_z)-(\sin^3\theta\cos\theta)\phi_1(\omega+\omega_z)]$$

(θ,φ). The absorption spectrum for any orientation of the chain axis with respect to the static field is obtained through Eqs. (11)–(15) for the two oscillating field configurations of interest. At high frequencies we know that it is essentially represented by $1/a_2$ (resonance configuration) and $1/a_3$ ("relaxation" configuration). In the first case, besides the main line corresponding to $\omega=\omega_z$, there is a half-field line occurring through the function $\phi(\Omega=\omega-2\omega_z)$ which peaks at $\Omega=0$. In the same way the relaxation spectrum is characterized by two secondary lines corresponding to $\phi(\omega-\omega_z)$ and $\phi(\omega-2\omega_z)$.

Now some interesting features will be discussed.

B. Symmetry in a zero static field

In zero applied dc field, the only relevant orientation parameter is the angle between the chain axis and the oscillating field. Symmetry conditions are implied in the following.

(i) If the chain axis is rotated in the $y0z$ plane (corresponding to $\varphi=90°$) Γ_x must be θ independent: the zero-field signal is a constant in this plane.

(ii) On the other side, for $\varphi=0°$, one has $\Gamma_x(\theta+90°)=\Gamma_z(\theta)$.

By setting $\omega_z=0$ the expressions for n, d, and n' become somewhat simpler,

$$n = 2a_3[a_1+b_0\cos(2\varphi)]+c_0^2[\cos(2\varphi)-1]\ ,$$

$$d = (a_1+b_0)[a_3(a_1-b_0)-c_0^2]\ ,$$

$$n' = a_1-b_0\ ,$$

with $b_0=e^{-2i\varphi}b_1$, $c_0=e^{-i\varphi}c_1$, being φ independent. Then, for $\varphi=90°$, one sees that, according to condition (i),

$$2d/n = a_1+b_0 = i\omega+\tfrac{9}{4}\omega_D^2\{(\cos^2\theta-\sin^2\theta)^2\phi_1(\omega) + \sin^2\theta\cos^2\theta[\phi_2(\omega)+3\phi_0(\omega)]\}$$

does not depend on θ, so that it follows necessarily that

$$\phi_0(\omega)=\phi_1(\omega)=\phi_2(\omega)=\phi(\omega)\ . \tag{24}$$

Such a result is especially interesting and is a generalization of the relation (21) previously established only for the exchange interaction. We note that it is implicitly assumed in usual treatments of high-frequency magnetic resonance in one-dimensional systems. In that case, however, the spectral density $\phi(\omega)$ is considered to be a function of θ through the cutoff frequency which is related to the linewidth: the static field breaks the symmetry. At

zero field $\phi(\omega)$ does not depend on θ.

We easily obtain the absorption amplitude for any orientation of c in the $y0z$ plane,

$$\Gamma'_x(\omega,\omega_z=0)=\langle S_x^2\rangle\frac{A_0}{\omega^2+A_0^2}\ , \tag{25}$$

with $A_0=\frac{9}{4}\omega_D^2\phi(\omega)$.

Now let $\phi=0°$. One has

$$\frac{n}{2d}=\frac{a_3}{a_3(a_1-b_0)-c_0^2}$$

$$\frac{n'}{d}=\frac{a_1-b_0}{a_3(a_1-b_0)-c_0^2}\ .$$

The change of θ into $\theta'=\theta+90°$ leaves c_0^2 unchanged while

$$a_1(\theta)-b_0(\theta)=a_3(\theta')\ ,$$

$$a_1(\theta')-b_0(\theta')=a_3(\theta)\ .$$

With these relations we see that condition (ii) is fulfilled.

For any orientation of c in the $x0z$ plane we have

$$\Gamma'_x(\omega,\omega_z=0)=\langle S_x^2\rangle\frac{A_0\cos^2\theta}{\omega^2+A_0^2}\ . \tag{26}$$

If the oscillating field was directed along 0z the absorption should be

$$\Gamma'_z(\omega,\omega_z=0)=\langle S_z^2\rangle\frac{A_0\sin^2\theta}{\omega^2+A_0^2}\ . \tag{27}$$

These two last relations are, of course, modified by inclusion of the interchain interactions in the model.

C. Some general properties

The absorption is given in terms of the function values $\phi(\Omega)$ with $\Omega=\omega$, $\omega\pm\omega_z$, and $\omega\pm2\omega_z$. In the high-temperature limit ($\hbar\omega\ll kT$), one has $\phi(-\Omega)=\phi(\Omega)$. Other results are

$$\Gamma(\omega,-\omega_z)=\Gamma(\omega,\omega_z)\ ,$$

$$\Gamma(-\omega,\omega_z)=\Gamma^*(\omega,\omega_z)\ .$$

It is to be noted that n' and d (and Γ_z) do not depend on φ, while n may be split into a φ-dependent term and another one with a 2φ periodicity.

For $\theta=0°$ there is no φ dependence, in agreement with Eq. (19). This is obvious in view of the fact that polarization effects are caused by nonsecular terms of the dipolar interaction.

D. The polarization effect

For our orientation of interest, $\theta=90°$, one has

$$\Gamma_x=\frac{\langle S_x^2\rangle}{2}\frac{a_1+a_2+b_1+c_2}{a_1a_2-b_1c_2} \tag{28}$$

with

$$a_1=i(\omega+\omega_z)+(A/2)\ ,$$

$$a_2=i(\omega-\omega_z)+(A/2)\ ,$$

$$b_1=\frac{A}{2}e^{2i\varphi},\quad c_2=\frac{A}{2}e^{-2i\varphi}\ ,$$

and

$$A=\tfrac{9}{8}\omega_D^2[\phi(\omega+\omega_z)+\phi(\omega-\omega_z)]\ ,$$

coinciding with A_0 at zero dc field. The absorption profile is then

$$\Gamma'_x=\langle S_x^2\rangle\frac{A}{(\omega^2-\omega_z^2)^2+\omega^2A^2}(\omega^2\sin^2\varphi+\omega_z^2\cos^2\varphi)\ . \tag{29}$$

It corresponds exactly to the relations obtained in Sec. II by using Bloch equations, corresponding to $\varphi=0°$ [Eq. (3)] and 90° [Eq. (4)]. We can make the identification

$$1/T_{2y}\equiv A\ . \tag{30}$$

All the conclusions derived previously in Sec. II are valid again and we do not repeat them. In the calculation A was treated as a real parameter. In fact, at low frequencies its imaginary part A'' is quite negligible and otherwise gives rise to a small shift (known in the literature as the "dynamic shift").

We note that at zero field for $\varphi=0°$, one has $\Gamma_x(\omega_z=0)=\langle S_z^2\rangle/i\omega$, the same result being obtained for Γ_z with the static field being applied along the chain axis ($\theta=0°$). Thus if the oscillating field is applied along the chain axis the susceptibility $\chi(\omega)$ is zero at any frequency and can be taken as a reference. This property is maintained if one applies a static field also in the chain direction. On the other hand, since the line amplitude at resonance varies such as ω^{-1}, it is seen from Eq. (9) that, at low frequencies, $\chi''(\omega)$ tends towards a constant value $(1/kT)\langle S_x^2\rangle$.

Of course, experimental deviations to these properties imply the existence of other sources of dampings and allow their evaluation. This is the topic of Sec. IV E.

E. Additional sources of damping

We have so far considered intrachain dipolar interaction as the only cause of damping. Of course all nonspin conserving interactions must be taken into account. We refer here to the TMMC case. The crystalline field acting on the Mn^{2+} ion gives rise to a single-ion anisotropy which has presumably the same symmetry axis (the chain axis) as the intrachain dipolar coupling, and thus plays the same role. Other anisotropic exchange terms can be neglected. In fact, main contributions result from hyperfine interactions and interchain couplings. The hyperfine contributions to damping is isotropic and involves two-spin correlation functions. The interchain contribution is rather difficult to calculate with accuracy. A chain is surrounded by six equidistant neighboring chains. We can make a reasonable hypothesis by assuming that the resulting damping is nearly isotropic. As a consequence the "nondiagonal" b and c terms resulting from those interactions can be neglected. Let interchain

and hyperfine contributions be represented by B. We add B to the "diagonal" terms a_1, a_2, a_3. Just as in Sec. IV D we consider the polarization effect. For $\theta=90°$, $\varphi=0°$ the calculation yields

$$\Gamma_x=\langle S_x^2\rangle\frac{(A+B)(\omega_z^2+AB+B^2)+B\omega^2}{(\omega_z^2-\omega^2+AB+B^2)^2+\omega^2(A+2B)^2} . \quad (31)$$

This corresponds exactly to relation (7) in Sec. II if we made the substitution

$$A+B\rightarrow 1/T_{2y} \quad B\rightarrow 1/T_{2x} . \quad (32)$$

The phenomenologic model coincides thus exactly with the microscopic theory, the damping being split here into an intrachain contribution and an extraneous one.

F. Exponential relaxation

We consider the spin relaxation as being "exponential" if there is an identity between Eq. (7) obtained from Bloch equations and Eq. (11) derived from first principles. Thus the amplitude and the shape of the lines can be described by means of two damping rates. This is indeed the case for the linear chain of spins when the static field is perpendicular to the chain axis ($\theta=90°$), and one can determine a damping rate in the chain direction $1/T_{2c}=0$ and a damping rate in a perpendicular direction $1/T_{2t}=A$ (the latter being complex and variable through the frequency and field dependence of the spectral densities).

It may be asked whether the identity found for $\theta=90°$ can be generalized to any orientation of fields. Is the spectrum anisotropy of the linear chain of spins fully described by a single anisotropic damping parameter? Intuitively, the damping in a direction making an angle α with the chain axis should be, in the low-field–low-frequency range, $1/T_{2(\alpha)}=(1/T_{2t})\sin^2\alpha$. The identity holds for $\theta=0°$ if the damping is field independent (i.e., $1/T_{2t}=A_0$) but unfortunately it breaks down at other orientations. The spin relaxation does not occur exponentially, even for a zero applied static field. If it did, one should have

$$\Gamma(\omega,\omega_z=0)=\langle S_x^2\rangle\frac{1/T_{2x}}{\omega^2+(1/T_{2x})^2} . \quad (33)$$

T_{2x} being the damping rate in the oscillating field direction.

When the chain axis is varied in the $x0z$ plane, this relation cannot be identified with Eq. (26), owing to the $\cos^2\theta$ term. On the other hand, if the chain axis is varied in the $y0z$ plane, Eq. (33) is in agreement with Eq. (25). This is because the relaxation in the direction perpendicular to the chain is indeed exponential. A condition for exponential relaxation is $\Gamma_z=(\langle S_z^2\rangle/a_3)$: it is fulfilled for $\theta=90°$. Nevertheless, at low fields, the spectral densities of correlation functions can be treated as constants so that the full spectrum anisotropy can be determined from knowing $1/T_{2t}$ only, through the microscopic theory.

V. EXPERIMENTAL APPARATUS

Measuring broad lines at low frequencies is rather delicate since the line amplitude varies as ω^2, the square of the angular frequency. Difficulties were overcome by using large samples and a very sensitive spectrometer.

Single crystals of $(CH_3)_4NMnCl_3$ (TMMC) were grown by slow evaporation at 30 °C of a stoichiometric acidified aqueous solution of $MnCl_2\cdot 4H_2O$ and $(CH_3)_4NCl$. Samples weighing up to 6 g could be obtained.

The low-frequency spectrometer used in the present experiments works in the frequency range 15–250 MHz. The scheme of the setup is shown in Fig. 4. A resonator containing the sample is placed inside the air gap of an electromagnet (Varian, 9 in.). The radio-frequency oscillations in the resonator are sustained by the very loose inductive coupling of a broadband multistage amplifier. The signal is detected at the output of the last unsaturated amplifier stage.

The resonator is heavy and large, allowing stable temperature and mechanical rigidity. This leads to high performance: good frequency stability, high quality factor, and thus large sensitivity and good signal-to-noise ratio. At low frequencies (25 MHz) the resonator is a simple LC circuit. Near 200 MHz a helicoidal quarter wavelength resonator[13] is used. At intermediate frequencies, between 75 and 140 MHz, a tunable resonator was built up (Fig. 5). Here the wrapped length of the helicoidal conductor is non-negligible compared to the wavelength, and this conductor is charged at its free end through an adjustable capacitor. With these resonators the field B_1 is so much more homogeneous as the frequency is lower. At 200 MHz the field inhomogeneity over the sample bulk is about 30%.

The amplifier has three stages: a preamplifier with bandwidth 5–500 MHz and gain 29 dB; an intermediate stage with bandwidth 1.5–500 MHz, gain 27 dB, and power 300 mW; a power amplifier (1 W) with bandwidth 10–420 MHz and gain 26 dB. This last stage is used as a limiter (i.e., in saturating conditions), so that the reinjected power in the resonator remains constant. Attenuators reduce the total loop gain to about 70 dB in order to obtain the maximum allowable signal at the detector. After detection the signal is passed through a low-pass filter (bandwidth 1 Hz) and then feeds a recorder after compensation of the dc level.

When scanning the field one measures directly the absorbed energy variations in the resonator. The direct recording method is advantageous for the theoretical analysis and the comparison with formulas derived in preceding sections. The first experiments were carried out with the best filling factor (corresponding to the configuration $\mathbf{B}_1\|$ the chain axis $\mathbf{c}$). A signal-to-noise ratio as high as 150 should be achieved in this way at 25 MHz. Then the need of rotating the samples leads us to design new resonators (Fig. 6), but with a poorer signal-to-noise ratio. Besides the noise, the main sources of error are dc drifts and a slightly field-dependent absorption of the empty coil circuit.

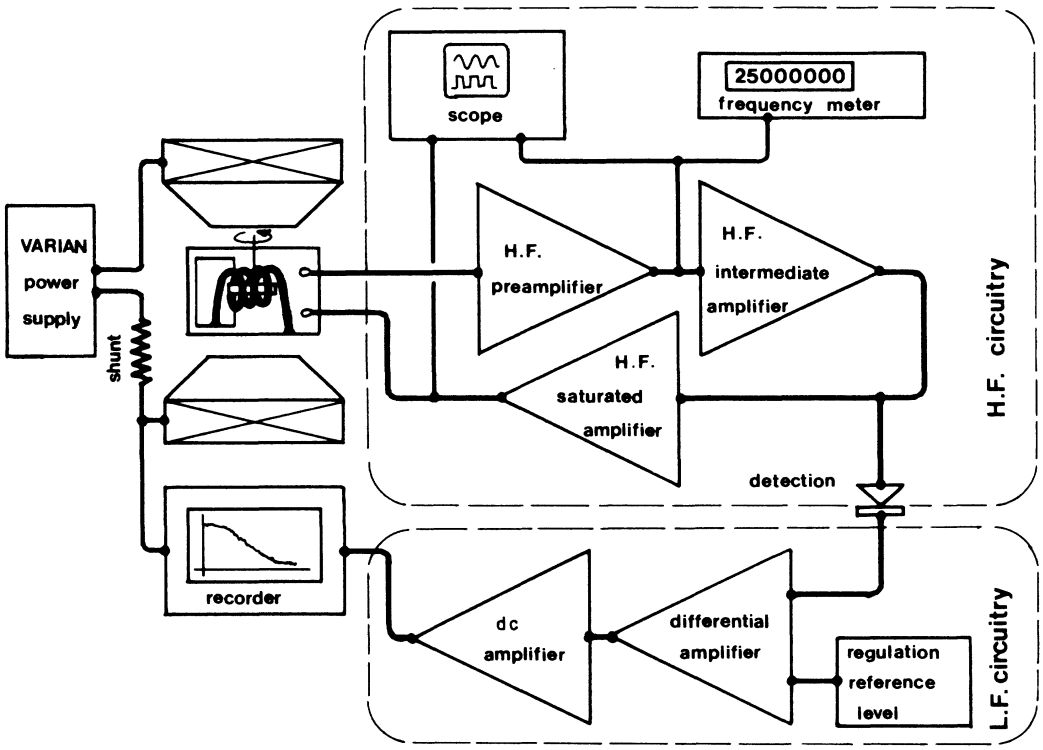

FIG. 4. Scheme of the low-frequency magnetic resonance spectrometer.

In order to improve the signal-to-noise ratio especially at lower frequencies, a magnetic modulation (at frequency 80 Hz) was incorporated and the derivative of the absorption line was yielded by a lock-in detector.

VI. EXPERIMENTAL RESULTS AND COMMENTS

Experimental evidence of the polarization effect was shown in a previous paper.[2] Here we compare in more detail the theory presented above with experimental results obtained in tetramethylammonium manganese chloride (TMMC):$(CH_3)_4NMnCl_3$. In this compound the distance between neighbor Mn spins within a chain is $c = 3.247$ Å while neighbor chains are separated by 9.151 Å. It can be inferred that the contribution of interchain interactions to the resonance spectrum is much smaller than intrachain ones. In other words the spin-damping coefficient along the chain $1/T_{2c}$ (which is zero in the case of fully isolated chains) is certainly much less than $1/T_{2t}$, the damping along a transverse direction. Our aim is to obtain accurate values for these damping terms. We recall that the oscillating field is chosen to be applied in the x direction while the static field is applied in the z direction.

Let us consider at first the parallel line, i.e., for the os-

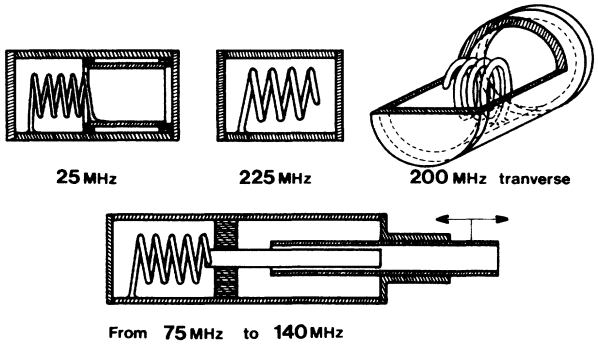

FIG. 5. Cross sections of the different resonators used in the experiments.

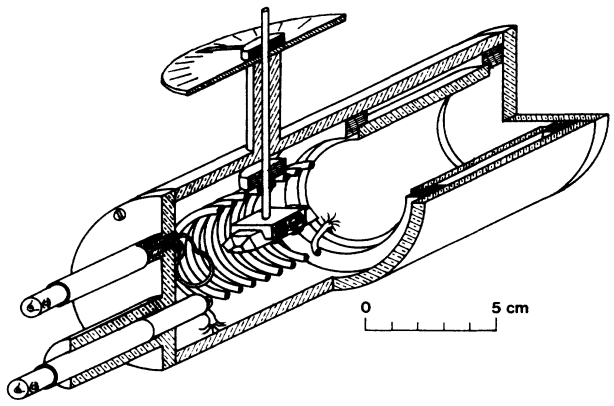

FIG. 6. Open view of a resonator with a sample rotation mechanism.

cillating field B_1 being directed along the chain axis. The theoretical absorption is given by Eq. (7) with $T_{2x}=T_{2c}$, $T_{2y}=T_{2t}$. One remarkable feature of the low-frequency spectrum is the important increase of Γ'_x characterized by a maximum value $\Gamma'_{x,\max}\simeq(\langle S_x^2\rangle/2\omega)$ [Eq. (6)], which is nearly independent of damping terms. Absolute values of Γ'_x can be measured by comparing the TMMC signal with the Lorentzian line yielded by a sample of free radical diphenyl picryl hydrozyl (DPPH). Let N and N' be the number of spins S and S', respectively, in TMMC and in DPPH samples. For DPPH one has

$$\Gamma'_x(\mathrm{DPPH})=\frac{\langle S_x^2\rangle}{2}\frac{\Delta\omega'}{(\omega-\omega_z)^2+(\Delta\omega')^2},$$

$\Delta\omega'$ being the half width at half-height of the line (in angular frequency units) and with

$$\langle S_x'^2\rangle=N'S'(S'+1)/3,\quad \langle Sx^2\rangle=NS(S+1)/3\ .$$

Signals were carefully measured at several frequencies, the samples being, in each case, in the same oscillating field distribution. Knowing the spin numbers from the weight of the samples, $S=\frac{5}{2}$, $S'=\frac{1}{2}$, one obtains for TMMC the reduced inverse amplitude $I_m^{-1}=\langle S_x^2\rangle/2\Gamma'_{x,\max}$, which should be equal to ω. Results are plotted in Fig. 7. In fact Eq. (6) is valid in the frequency range $1/T_{2c}<\omega\ll 1/T_{2t}$, in good agreement with experimental results.

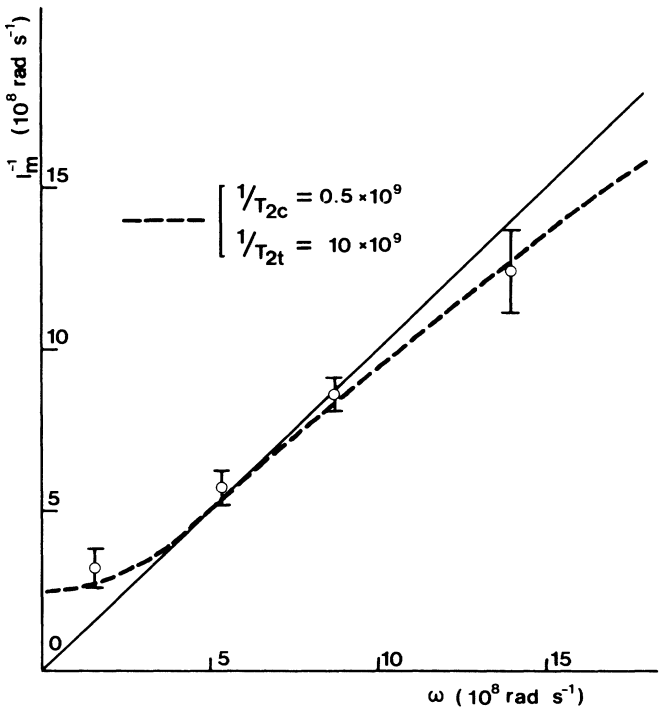

FIG. 7. Reduced inverse amplitude of the resonance absorption in TMMC as a function of the frequency. The circles are experimental points. The solid line corresponds to Eq. (6). The dashed line is obtained from Eq. (7) with the damping parameters $1/T_{2c}=5.0\times10^8$ rad s^{-1} and $1/T_{2t}=10^{10}$ rad s^{-1}.

The field corresponding to maximum absorption, hereafter called the "resonance field" is, to a high degree of accuracy, given by the following relation:

$$\omega_z(\mathrm{res})=\frac{1}{T_{2t}}\left[\omega-\frac{1}{T_{2c}}\right]+\frac{\omega}{T_{2c}}\ . \tag{34}$$

It becomes zero for a value of ω somewhat below $1/T_{2c}$. Near this value, it can be shown that $\omega_z(\mathrm{res})$ is extremely sensitive to $1/T_{2c}$ but only weakly to $1/T_{2t}$. The value of $1/T_{2c}$ can be obtained in this way. Experimental data are shown in Fig. 8 and compared with Eq. (34). A good fit is obtained with $1/T_{2c}=5\times10^8$ rad s^{-1} and $1/T_{2t}=10^{10}$ rad s^1. These values are also in good agreement with the experimental data of Fig. 7.

Now we compare the parallel line to the perpendicular one. Figure 9 shows the derivative absorption spectrum in TMMC measured at a frequency of 25 MHz for these two configurations. Both lines have approximately the same width but the ratio of their maximum amplitude is about 18, approximately T_{2c}/T_{2t}. The theoretical points are obtained by derivating Eq. (7) with respect to ω_z and using $T_{2x}=T_{2t}$, $T_{2y}=T_{2c}$ for the perpendicular line. The agreement is good considering the weakness of the perpendicular signal which is superimposed to a parasitic

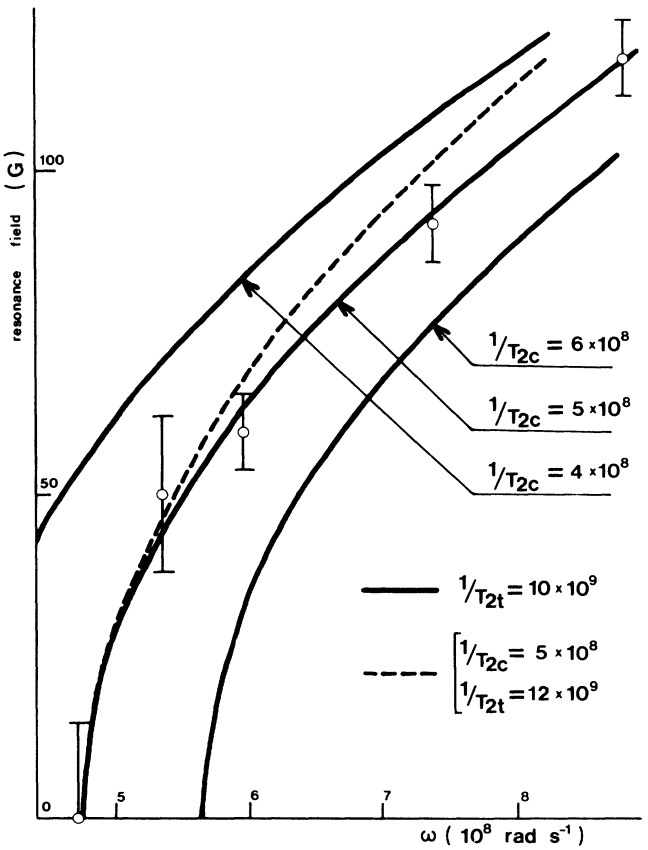

FIG. 8. Resonance field in TMMC as a function of the frequency. The circles are experimental points. The lines correspond to Eq. (34), with several values of the damping parameters.

signal.

Let us now consider other orientations. Experimentally we first vary the chain axis orientation in the $(\mathbf{B}_1,\mathbf{B}_0)$ or the $x0z$ plane (using spherical coordinates, this is the $\varphi=0°$ plane). At 25 MHz one observes a marked variation of the derivative line (Fig. 10), the spectrum flattening as the angle θ between the chain axis and $\mathbf{B}_0$ is reduced. For $\theta=0°$ one can again describe the spectrum by means of the phenomenological theory: the spectrum is given by Eq. (2) with $T_2=T_{2t}$, as long as the damping can be considered as a constant. For other orientations we have shown in Sec. IV F that the phenomenologic model is no more valid. Nevertheless we tentatively compare the amplitude and shape of the lines with Eq. (7).

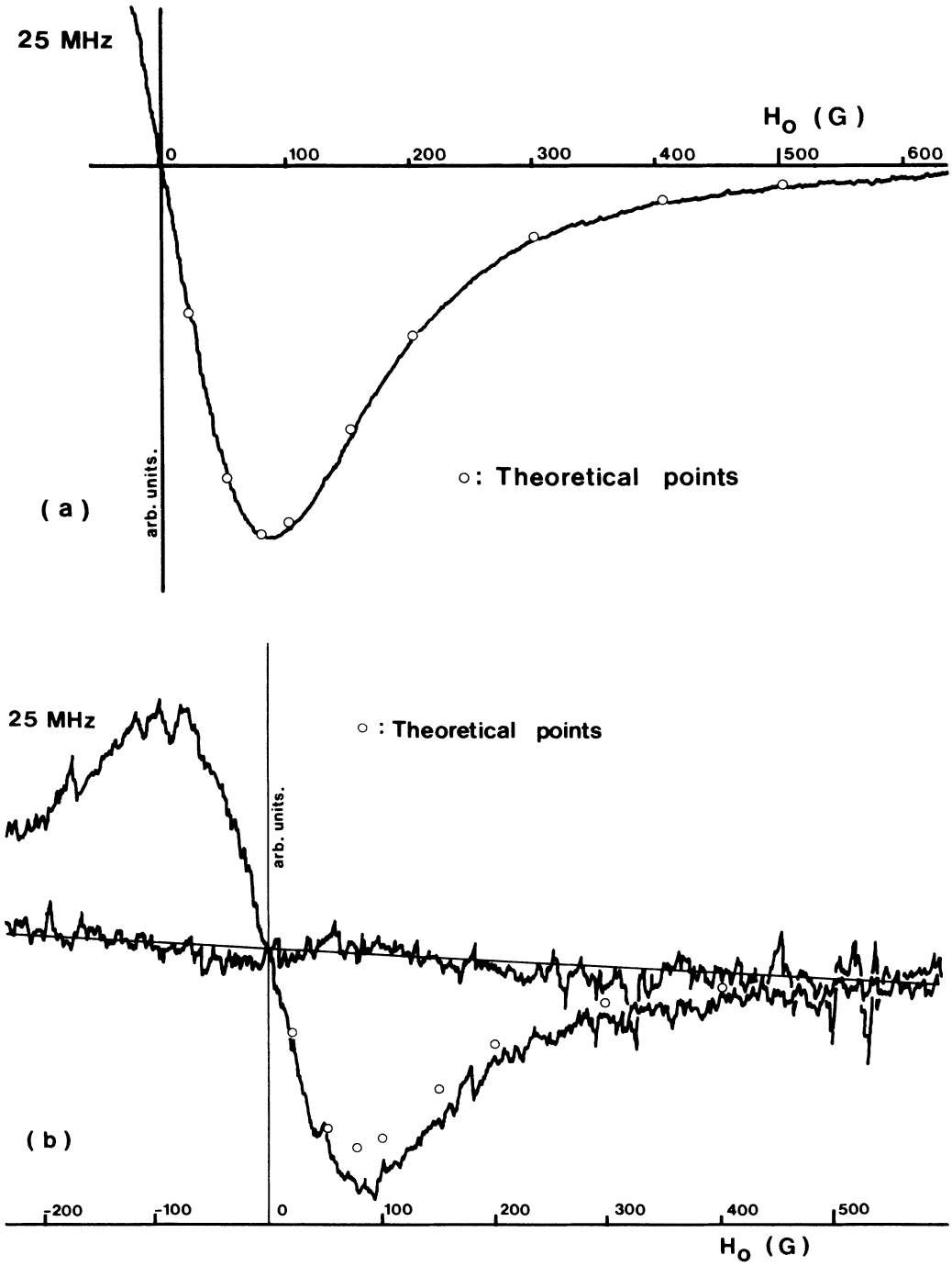

FIG. 9. Derivative absorption spectrum in TMMC at 25 MHz for two oscillating-field polarizations. (a) Parallel to the chain axis; (b) perpendicular to the chain axis. The static field is perpendicular to the chain axis and to the oscillating field. In (b) the gain has been increased by a factor of 10 and the baseline has been plotted together with the signal. The circles are theoretical points obtained with the damping parameters $1/T_{2c}=5.0\times10^8$ and $1/T_{2t}=10^{10}$. The amplitudes are scaled on the maximum signal in the parallel configuration.

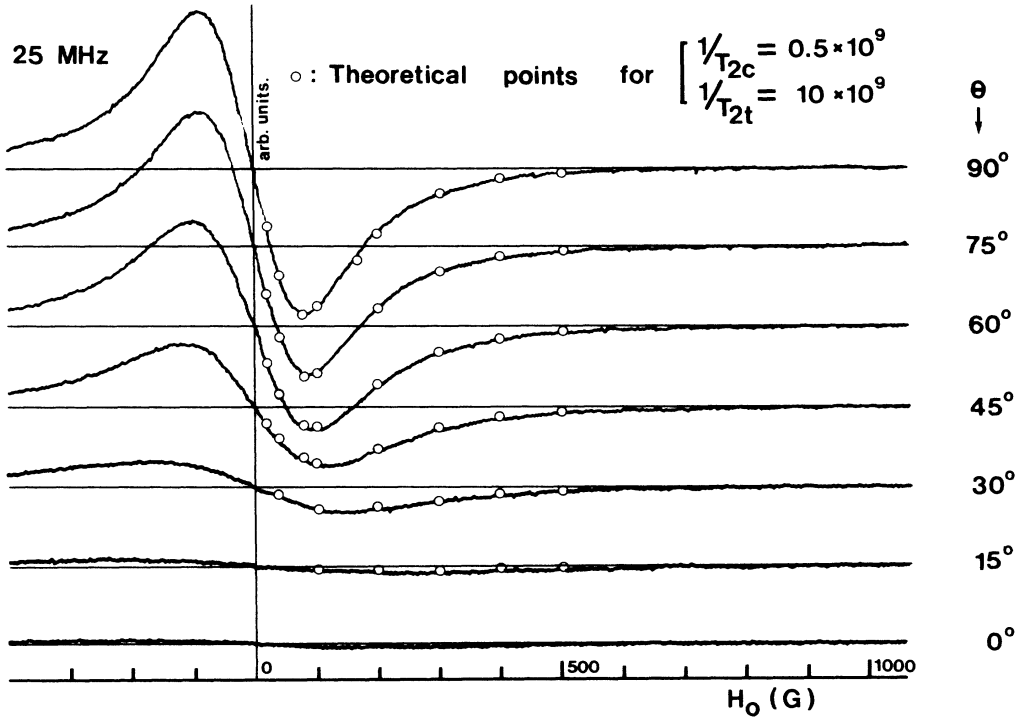

FIG. 10. Derivative lines in TMMC at 25 MHz for several orientations of the chain axis in the $(\mathbf{B}_0,\mathbf{B}_1)$ plane. θ is the angle between the chain axis and the static field $\mathbf{B}_0$. The amplitudes are scaled on the maximum signal for $\theta=90°$.

Let us choose $\theta=60°$. The spectrum should be described by $1/T_{2y}=1/T_{2t}$ and by $1/T_{2x}$ which has to be obtained from the experimental line. A value of $1/T_{2x}=8\times10^8$ rad s^{-1} gives a good fit for the line shape but not for the amplitude: we compare the maximum amplitudes of the derivative lines, respectively, for $\theta=90°$ and $\theta=60°$; it is found that the theoretical ratio between them is 2, while the experimental ratio is only 1.4. It is necessary to use the theory presented in Secs. III and IV, especially Eqs. (11)–(13), Table I, and Eq. (24). The polarization effect was described with parameters A (intrachain contribution) and B (interchain contribution). The low-frequency–low-field condition allows us to write $\phi(\Omega)\simeq\phi(0)$ so that A is a constant appearing in all terms of Table I. The correspondence with the previous (phenomenologic) description is given by

$$B=1/T_{2c},\quad A=1/T_{2t}-1/T_{2c}\ .$$

The agreement with theoretical points is very good, not only for shapes but also for amplitudes (all amplitudes have been scaled to the maximum value of the $\theta=90°$ result). Thus, we distinguish the intrachain contribution $A=9.5\times10^9$ rad s^{-1} and the interchain one (the hyperfine contribution is supposed to be negligible here) $B=0.5\times10^9$ rad s^{-1}.

If the chain orientation is varied in the plane $y0z$ perpendicular to $(\mathbf{B}_1,\mathbf{B}_0)$, corresponding to $\varphi=90°$, there is another interesting feature: the signal at zero dc field must be a constant, owing to the symmetry of the system. This is indeed experimentally verified (Fig. 11). The agreement with theory is also very good, except when the dc field orientation is near the chain axis. The reason is that, in this case, spin-damping coefficients can no longer be considered as constants. In fact, we have shown in Sec. IV that spin dampings are field and frequency dependent through the spectral densities $\phi(\Omega)$, where Ω takes the values ω, $\omega\pm\omega_z$, $\omega\pm2\omega_z$. While sweeping the dc field through the line, the spin damping is thus varying, The spectral densities are expected to vary appreciably for $\Omega\gtrsim\omega_c$, the cutoff frequency. In zero-applied dc field, ω_c is isotropic and presumably of the order of the maximum linewidth (in field unit, 500 G or larger). This explains why the deformation occurs for broader lines, near $\theta=0°$. The analysis is intricate because ω_c is a function of the amplitude and the orientation of the dc field.

In zero dc field the absorption in the resonance configuration $(\mathbf{B}_1\perp\mathbf{B}_0)$ and the absorption in the relaxation configuration $(\mathbf{B}_1\|\mathbf{B}_0)$ are, of course, the same. They are described by the same damping term. It results that $\Gamma_x(\theta+90°)=\Gamma_z(\theta)$. This means that $1/T_{2c}$ coincides with the relaxation rate $1/T_{1c}$ measured along the chain axis, in the same way $1/T_{2t}$ coincides with the relaxation rate $1/T_{1t}$ measured in the transverse direction. This identity is broken when a dc field is applied in the z direction, T_1 and T_2 varying differently. Thus the quantities we measured correspond to the low-field–low-frequency $1/T_1$ values. We discovered recently that some years ago absorption measurements with relaxation configuration were performed in TMMC by Van Noort.[14] The "characteristic frequency" studied by this author corresponds in fact to $1/T_1$. He obtained at zero dc field, re-

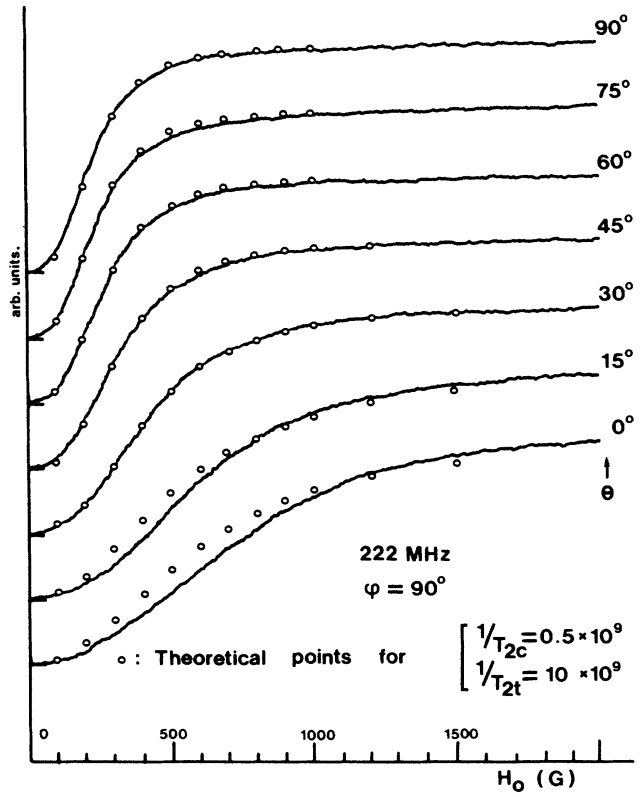

FIG. 11. Absorption lines in TMMC at 225 MHz for several orientations of the chain axis in the plane perpendicular to the oscillating field B_1. θ is the angle between the chain axis and the static field. The amplitudes are scaled on the maximum signal for $\theta=90°$. For the sake of clarity the signal baselines for successive orientations are shifted by a constant value. The experimental zero-field signal amplitude is isotropic in this plane.

spectively, 4.9×10^8 for the high-frequency field parallel to the c axis and 9.2×10^9 in the perpendicular case. This is in good agreement with our low-field results

$$1/T_{2c}=(5\pm0.2)\times10^8 \text{ rad s}^{-1} ,$$

$$1/T_{2c}=(10\pm0.5)\times10^9 \text{ rad s}^{-1} .$$

The interchain contribution B was evaluated by Lauer and Benner.[15] They measured the linewidth in Cu-doped TMMC at the magic angle and did not verify at very high frequencies the expected relation $\Delta\omega\propto\omega^{-1/2}$ resulting from spin diffusion. They explained this by the influence of the interchain contribution. They deduced a value as high as 70 G in pure TMMC. This is more than twice the value we obtained at low frequencies. It is possible that Lauer and Benner did not probe at the high frequencies used (up to 44×10^{10} rad s^{-1}) the diffusion zone of the correlation function. In fact, if one considers two-spin correlation functions, the diffusive processes do not establish before a time 10^{-12} s (Ref. 16) and this situation probably holds for the function $\varphi_{KT}(t)$ considered here. Doping delays the onset of diffusive behavior. Not let us compare the value found for A with the theoretical one. We calculate $A\simeq A_0=\frac{9}{4}\omega_D^2\phi(0)$ with

$$\phi(0)=\int_0^\infty \varphi_{KT}(t)e^{-i\omega_c t}dt .$$

If we use the usual spin decoupling, φ_{KT} is found to follow a diffusive law for times $D^{-1}\ll t<1/\omega_c$,

$$\varphi_{KT}(\text{diff})\simeq\frac{8}{3}\frac{\zeta^2(3)S(S+1)}{(2\pi Dt)^{1/2}} .$$

This gives the main contribution to $\phi(0)$. Here the spin-diffusion coefficient D is expressed in frequency units, $D\simeq6.9\times10^{12}$ rad s^{-1} in TMMC,[16] $\zeta(x)=\sum_{n=1}^{\infty}n^{-x}$, and $\omega_D=\hbar\gamma^2/c^3=9.5\times10^9$ (rad s^{-1}). The cutoff frequency is of the order of the maximum linewidth (i.e., for $\theta=0°$). Let us choose $\omega_c=10^{10}$ rad s^{-1}. We obtain $A=2.0\times10^{10}$ rad s^{-1}, approximately twice the experimental value. In fact the disagreement is not surprising since it has been observed by a number of researchers,[8,9] but the reasons for the discrepancy are not clear. Cheung *et al.*[12] tried to explain it by a temperature effect and by relaxing the cutoff condition, $\omega_c\simeq\alpha\Delta\omega$, where α is chosen between 1.5 and 2. However the temperature dependence is not shown by experiments at the magic angle.[17] Other invoked causes are the failing of the spin-decoupling procedure or the existence of an anisotropic single-ion term, with the same symmetry as the dipolar term.

Measurements by Siegel and Lagendijk[18] have shown that, for the $\theta=90°$ orientation, the linewidth increases slightly as the frequency is raised from 2 to 18 GHz. These authors explained their results on the basis of a mode-coupling theory. In fact this effect is easily accounted for by Eq. (29).

VIII. CONCLUSION

We have shown here that magnetic resonance spectra at low frequencies (i.e., of the same order of the linewidth or lower than the linewidth) are incorrectly described by the usual theories.

From a phenomenologic point of view, Bloch equations must be generalized by including two damping rates terms: a parallel one ($1/T_{2x}$), corresponding to the oscillating-field polarization direction $\mathbf{B}_1$, and a perpendicular one ($1/T_{2y}$) corresponding to the direction perpendicular both to $\mathbf{B}_1$ and to the static field $\mathbf{B}_0$. In highly anisotropic systems these terms may be very different from each other. The limiting case is attained with the isolated linear chain of spins: the damping rate in the chain direction is zero. As pointed out in a previous Letter[2] this is in relation with the total spin conservation. At high frequencies the spectrum may be, in fact, described by a single damping term which is the average of $1/T_{2x}$ and $1/T_{2y}$. But when the frequency is lowered, the spectrum becomes more and more sensitive to the parallel damping term. When studying the spectrum anisotropy, the oscillating field polarization direction becomes indeed a relevant experimental parameter, allowing the measurement of the damping term in each direction. In particular, at low frequencies, the zero-field absorption becomes proportional to the parallel damping time.

A microscopic theory which describes correctly all

these features incorporates all nondiagonal components of the frequency-dependent tensor. The usual theory takes into account diagonal terms only. This is equivalent to an averaging of the parallel and the perpendicular damping rates.

In the case of an isolated chain of spins, a perfect correspondence between phenomenologic and microscopic theories is observed for preferred orientations of magnetic fields. If the static field is parallel to the chain axis or perpendicular to it, the spectrum is described by means of two damping terms; in the chain direction ($1/T_{2c}=0$) and in the perpendicular direction ($1/T_{2t}$). The microscopic theory allows the calculation of $1/T_{2t}$ and shows that it is dependent on the static field amplitude.

In real systems one has to take into account interchain interactions. In TMMC they are mainly dipolar, implying here also four-spin correlation functions, but with two spins belonging to a chain and the others to a neighboring one. We have not calculated the corresponding contribution: we rather assumed that it was isotropic and deduced its value from experiment.

The important low-frequency effects observed in TMMC result from the high ratio of intrachain-to-interchain dipolar interactions, caused by geometric reasons. We remark that T_{2c}/T_{2t} is nearly equal to the inverse cube of the ratio of the intrachain-to-interchain ion separation. On the contrary, the compound $CsMnCl_3 \cdot 2H_2O$ is characterized by good one-dimensional exchange properties but the structural lattice is rather three dimensional: only very weak polarization effects are observed in this case.[19]

Low-frequency ESR experiments are not commonly performed since poor signal-to-noise ratio is expected. However such studies provide significant information on anisotropic systems. In TMMC measurements were made easier in spite of broad linewidths because we were able to grow large crystals and the signal was enhanced by the polarization effect. In fact our apparatus sensitivity allows studies in less favorable samples (with lower spin value or lower one-dimensional character).

ACKNOWLEDGMENT

Institut d'Electronique Fondamentale is a Laboratoire associé au Centre National de la Recherche Scientifique.

APPENDIX: DERIVATION OF THE MAGNETIC RESONANCE LINE PROFILE

The starting point is the evolution equation

$$\frac{\partial S_\alpha}{\partial t}=\frac{i}{\hbar}[H,S_\alpha(t)]\equiv iLS_\alpha(t)\ . \tag{A1}$$

The kinetic equations characterizing the spin dynamics are deduced by using a method introduced by Zwanzig.[20] The relevant variables of the system being (S_+,S_-,S_z) one defines a projection operator P (Ref. 20) such that

$$PX=\frac{S_+\langle S_-X\rangle}{\langle S_-S_+\rangle}+\frac{S_-\langle S_+X\rangle}{\langle S_+S_-\rangle}+\frac{S_z\langle S_zX\rangle}{\langle S_z^2\rangle}\ . \tag{A2}$$

The following relations are especially useful:

$$PS_\alpha=S_\alpha$$

$$\langle S_\alpha Pf(t)\rangle=\langle S_\alpha f(t)\rangle\ ,$$

$f(t)$ being any time function.

It must be understood that these relations are exact as far as the crossed static correlations $\langle S_+S_z\rangle$, $\langle S_+S_+\rangle\ldots$, are zero, which is expected in the following.

After some algebraical manipulations it can be shown that

$$\frac{\partial}{\partial t}PS_\alpha(t)=iPL\{PS_\alpha(t)+(1-P)S_\alpha(t)\}$$

with

$$(1-P)S_\alpha(t)=e^{i(1-P)Lt}(1-P)S_\alpha(0)+i\int_0^t e^{i(1-P)L(t-\tau)}(1-P)LPS_\alpha(\tau)d\tau$$

so that

$$\frac{\partial}{\partial t}G_{\alpha\beta}(t)=i\langle S_\alpha LPS_\beta(t)\rangle-\int_0^t\langle S_\alpha Le^{i(1-P)L(t-\tau)}(1-P)LPS_\beta(\tau)\rangle d\tau\ .$$

Now we replace $PS_\beta(t)$ by using Eq. (A2). Usually, here also, correlation terms which are zero at zero time are neglected. However in our derivation all terms will be considered.

A set of coupled equations is obtained,

$$\frac{\partial}{\partial t}G_{\alpha\beta}(t)=\sum_\gamma i\omega_{\alpha\gamma}G_{\gamma*}\beta(t)-\int_0^t d\tau\, k_{\alpha\gamma}(t-\tau)\Gamma_{\gamma^*\beta}(\tau)\ , \tag{A3}$$

with the characteristic frequencies

$$\omega_{\alpha\beta}=\langle S_\alpha LS_\beta\rangle/\langle S_\beta S_\beta^*\rangle \tag{A4}$$

and the so-called memory functions

$$k_{\alpha\beta}(t)=\langle S_\alpha L(1-P)e^{i(1-P)Lt}(1-P)LS_\beta\rangle/\langle S_\beta S_\beta^*\rangle\ . \tag{A5}$$

By Laplace transforming Eq. (A3) we get

$$i\omega\Gamma_{\alpha\beta}(\omega)=\langle S_\alpha S_\beta\rangle+[i\omega_{\alpha\beta}-K_{\alpha\gamma}(\omega)]\Gamma_{\gamma^*\beta}(\omega)\ . \tag{A6}$$

Let X, Y, Z be, respectively, $\Gamma_{+-}(\omega)$, $\Gamma_{--}(\omega)$, $\Gamma_{z-}(\omega)$ and X', Y', Z' be, respectively, $\Gamma_{-+}(\omega)$, $\Gamma_{++}(\omega)$, $\Gamma_{z+}(\omega)$. The desired function is

$$\Gamma_x(\omega)=\tfrac{1}{4}(X+Y+X'+Y')\ .$$

The X, Y, Z functions are obtained from the coupled equations (A6), which can be exactly solved as

$$a_1X=b_1Y+c_1Z+\langle S_+S_-\rangle\ ,$$

$$a_2Y=b_2Z+c_2X\ ,$$

$$a_3Z=b_3X+c_3Y\ .$$

The coefficients $a_1,a_2\ldots$, are given in Table II as a function of the characteristic frequencies and the memory functions. In the same way, X', Y', and Z' can be obtained from the system

$$a_2X'=c_2Y'+b_2Z'+\langle S_+S_-\rangle\ ,$$

$$a_1Y'=c_1Z'+b_1X'\ ,$$

$$a_3Z'=c_3X'+b_3Y'\ .$$

Finally we get

$$\Gamma_x(\omega)=\frac{\langle S_+S_-\rangle}{4}\frac{n}{d}\ , \tag{A7}$$

TABLE II. Theoretical expressions of the line-shape parameters in the general case. $K_{\alpha\beta}$ are the memory functions and $\omega_{\alpha\beta}$ are the characteristic frequencies.

$a_1=i(\omega-\omega_{+-})+K_{+-}$	$a_2=i(\omega-\omega_{-+}+K_{-+}$
$a_3=i(\omega-\omega_{zz})+K_{zz}$	$b_1=i\omega_{++}-K_{++}$
$b_2=i\omega_{-z}-K_{-z}$	$b_3=i\omega_{z-}-K_{z-}$
$c_1=i\omega_{+z}-K_{+z}$	$c_2=i\omega_{--}-K_{--}$
$c_3=i\omega_{z+}-K_{z+}$	

with

$$n=a_3(a_1+a_2+b_1+c_2)+(b_2-c_1)(b_3-c_3)\ , \tag{A8}$$

$$d=a_1a_2a_3-a_1b_2c_3-a_3b_1c_2 -b_1b_2b_3-a_2b_3c_1-c_1c_2c_3\ . \tag{A9}$$

If the oscillating field is polarized along the z axis—the so-called relaxation configuration—the absorption line profile is given by the Laplace transform of $\langle S_zS_z(t)\rangle$. The reasoning is quite the same as before and we then get

$$\Gamma_z(\omega)=\langle S_z^2\rangle\frac{n'}{d'} \tag{A10}$$

with

$$n'=a_1a_2-b_1c_2\ . \tag{A11}$$

All other cases of orientation can, of course, be calculated in this way.

[1]R. Kubo, M. Toda, and N. Hashitsume, *Statistical Physics II* (Springer-Verlag, Berlin, 1985), p. 130.

[2]S. Clément, E. Bize, and J. P. Renard, Phys. Rev. Lett. **53**, 2508 (1984).

[3]Y. Natsume, F. Sasagawa, M. Toyoda, and I. Yamada, J. Phys. Soc. Jpn. **48**, 50 (1980).

[4]R. Kubo and K. Tomita, J. Phys. Soc. Jpn. **9**, 888 (1954).

[5]Similar equations were obtained independently by H. Benner, M. Brodehl, H. Seitz, and J. Wiese, J. Phys. C **16**, 6011 (1983).

[6]C. Cohen-Tannoudji, B. Diu, and F. Laloë, *Mécanique Quantique* (Hermann, Paris, 1973), Chap. 13.

[7]R. E. Dietz, F. R. Merritt, R. Dingle, D. Hone, B. G. Silbernagel, and P. M. Richards, Phys. Rev. Lett. **26**, 1186 (1971).

[8]G. F. Reiter and J. P. Boucher, Phys. Rev. B **11**, 1823 (1975).

[9]A. Lagendijk, Phys. Rev. B **11**, 1322 (1978).

[10]R. Kubo, *Lectures in Theoretical Physics* (Interscience, New York, 1959), Vol. I.

[11]J. P. Boucher, M. Ahmed-Bakheit, M. Nechtschein, M. Villa, G. Bonera, and F. Borsa, Phys. Rev. B **13**, 4098 (1976).

[12]T. T. P. Cheung, Z. G. Soos, R. E. Dietz, and F. R. Merritt, Phys. Rev. B **17**, 1266 (1978).

[13]W. W. Macalpine and R. O. Schildknecht, Proc. Inst. Radio Eng. **47**, 2099 (1959).

[14]H. L. Van Noort, Ph.D. thesis, Kamerlingh Onnes Laboratory, University of Leiden, 1977 (unpublished).

[15]C. Lauer and H. Benner, Phys. Rev. B **23**, 1339 (1981).

[16]N. A. Lurie, D.L. Huber, and M. Blume, Phys. Rev. B **9**, 2171 (1974).

[17]E. Siegel, H. Mosebach, N. Pauli, and A. Lagendijk, Phys. Lett. **90A**, 309 (1982).

[18]E. Siegel and A. Lagendijk, Solid State Commun. **32**, 561 (1979).

[19]E. Bize, S. Clément, and J. P. Renard, Proceedings of the International Conference on Magnetism, Paris, 1988 [J. Phys. (Paris) (to be published)].

[20]R. Zwanzig, *Lectures in Theoretical Physics* (Interscience, New York, 1961), Vol. III; D. Kivelson and K. Ogan, Adv. Magn. Res. **7**, 71 (1974).